

A one-pot method to prepare transparent poly(methyl methacrylate)/montmorillonite nanocomposites using imidazolium-based ionic liquids

Hong Xu,^{a,b} Fangfang Tong,^c Jian Yu,^{a*} Lixiong Wen,^c Jun Zhang^{a*} and Jiasong He^a

Abstract

Poly(methyl methacrylate) (PMMA)/montmorillonite (MMT) nanocomposites were prepared by a new one-pot technique, where the hydrophilic Na-MMT layers were decorated with hydrophobic 1-dodecyl-3-methylimidazolium hexafluorophosphate ($C_{12}mimPF_6$) ionic liquid *in situ* during melt blending with PMMA and intercalation of polymer chains took place subsequently. The *in situ* modification and intercalation of Na-MMT were confirmed using X-ray diffraction and transmission electron microscopy. The combination of the compatible $C_{12}mimPF_6$ with PMMA and the good dispersion of MMT layers at the nanoscale rendered the resultant PMMA/MMT nanocomposites with improved optical transparency, thermal stability and mechanical properties.

© 2012 Society of Chemical Industry

Keywords: ionic liquids; nanocomposite; PMMA; transparency

INTRODUCTION

Polymer/layered silicate nanocomposites have attracted a great deal of attention due to the remarkable properties enhancement,^{1–5} including mechanical properties, thermal stability, flame retardancy and barrier properties. Such nanocomposites can be prepared by dispersing silicate layers in a polymeric matrix, using three main methods: *in situ* polymerization,^{6–10} solution blending^{11–15} and melt blending.^{16–20}

Montmorillonite (MMT) is one of the most widely employed layered silicates, because of its natural abundance together with high stiffness and swelling behavior.^{21–23} The most promising feature of MMT is that its interlayer spacing can be extensively expanded, which is necessary for the preparation of polymer/layered silicate nanocomposites. Nevertheless, the dispersion of MMT in polymer matrices is impeded by the incompatibility between the hydrophilic MMT surface and hydrophobic polymers. Thus the organic modification of MMT by ion-exchange reaction between pristine MMT and organic surfactant molecules is of great significance, which increases the interlayer spacing and the organophilicity of the MMT layers and consequently enhances their compatibility with organic polymers.

Conventionally, alkylammonium surfactants are widely used to prepare organophilic MMT using standard ion-exchange techniques.^{10,17,24} However, the MMT usually needs a long time (hours or even days) to be organically modified before it can be blended with polymers. Furthermore, alkylammonium-treated MMT has low thermal stability, resulting from the low decomposition temperature of the alkylammonium cations. By comparison, imidazolium cations are more thermally stable.^{25,26}

Alkylimidazolium-treated MMT has onset and maximum decomposition temperatures about 100 °C higher than those of the corresponding alkylammonium-treated MMT.²⁷ Alkylimidazolium-based ionic liquids, which are organic salts with melting points below 100 °C, have been the focus of many reports on the organic modification of MMT.^{26–33} Alkylimidazolium-based ionic liquids are reported as potential functional additives for improving the material properties of polymers, because of their non-volatility, non-flammability, recyclability, thermal stability, unique solvating ability, adjustable hydrophilicity and high ionic conductivity.²⁹ For example, 1-butyl-3-methylimidazolium hexafluorophosphate is found to be an effective plasticizer for poly(methyl methacrylate) (PMMA) to modulate the glass transition temperature (T_g) over a widened temperature range and improve the thermal stability of PMMA in comparison to traditional dioctylphthalate plasticizer.^{34,35}

* Correspondence to: Jian Yu and Jun Zhang, Beijing National Laboratory for Molecular Sciences (BNLMS), Key Laboratory of Engineering Plastics, Joint Laboratory of Polymer Science and Materials, Institute of Chemistry, Chinese Academy of Sciences, Beijing 100190, PR China.
E-mail: yuj@iccas.ac.cn; jzhang@iccas.ac.cn

a Beijing National Laboratory for Molecular Sciences (BNLMS), Key Laboratory of Engineering Plastics, Joint Laboratory of Polymer Science and Materials, Institute of Chemistry, Chinese Academy of Sciences, Beijing 100190, PR China

b Graduate School, Chinese Academy of Sciences, Beijing 100039, PR China

c State Key Laboratory of Organic-Inorganic Composites, Beijing University of Chemical Technology, Beijing 100029, PR China

In the study reported here, an ionic liquid (1-dodecyl-3-methylimidazolium hexafluorophosphate, $C_{12}mimPF_6$) composed of an imidazolium cation with a long alkyl group and hexafluorophosphate anion was used as a hydrophobic modifier for MMT and a plasticizer for PMMA as well. Due to the unique compatibility of alkylimidazolium-based ionic liquids with MMT and PMMA, a new one-pot method to prepare polymer/MMT nanocomposites was proposed and experimentally verified. By this method, hydrophilic MMT could be organically modified with $C_{12}mimPF_6$ and further intercalated with PMMA during melt blending, eliminating the time-consuming process of organic modification of MMT in an advance step. The intercalation and even exfoliation of MMT layers were confirmed using X-ray diffraction (XRD) and transmission electron microscopy (TEM). Furthermore, the high light transmittance of the nanocomposites obtained was validated using UV-visible spectroscopy, and the dynamic mechanical and thermal properties were characterized using dynamic mechanical analysis (DMA) and thermogravimetric analysis (TGA).

EXPERIMENTAL

Materials

PMMA was obtained from Aladdin Chemistry Co. Ltd (Shanghai, China). Pristine sodium MMT (Na-MMT) with a cation exchange capacity (CEC) of 90 mmol (100 g)⁻¹ was purchased from Qinghe Chemical Factory (Hebei, China). 1-Dodecyl-3-methylimidazolium bromide ($C_{12}mimBr$) and $C_{12}mimPF_6$ were supplied by Lanzhou Institute of Chemical Physics, Chinese Academy of Sciences. Organic-MMT, which had been organically modified using *N,N*-dimethyl-*N,N*-octadecylammonium chloride, designated AMMT, was supplied by Xi'an Changzhi Factory. All reagents were used as received.

Synthesis of nanocomposites

The nanocomposites were prepared using two methods: a one-pot melt method (OM) and a typical two-step melt intercalation (TM).^{16–20}

Preparation of nanocomposites by OM

Na-MMT was melt-blended with PMMA in the presence of $C_{12}mimPF_6$, which has potential as a multifunctional additive for polymer materials, without the need for organic modification in advance. PMMA was blended with $C_{12}mimPF_6$ and Na-MMT directly in a batch mixer (Haake RC90 Rheomix 600) at 200 °C. The rotator speed was 30 rpm for the initial 4 min, and then increased to 50 rpm for another 6 min. The samples were prepared with a $C_{12}mimPF_6$ content of 2.5% and various Na-MMT contents of 0, 0.5, 1 and 2 wt%, which are designated as OM-IL2.5, OM-MMT0.5-IL2.5, OM-MMT1-IL2.5 and OM-MMT2-IL2.5, respectively. A nanocomposite with a $C_{12}mimPF_6$ content of 5 wt% and Na-MMT content of 1 wt%, OM-MMT1-IL5, was also prepared.

Preparation of nanocomposites by TM

For comparison, Na-MMT was modified with $C_{12}mimBr$ in water using a standard ion-exchange technique to synthesize organophilic MMT ($C_{12}mim$ -MMT). An amount of 1.5 eq. of $C_{12}mimBr$ with respect to the CEC value of Na-MMT was used. The mixture was refluxed under stirring for 6 h. Then the treated MMT was filtered and washed with distilled water until no Br^- was detected. It was dried in vacuum and then ground to a fine powder in an agate mortar.

TM nanocomposites were prepared by melt-blending PMMA and $C_{12}mim$ -MMT under the same conditions as for OM nanocomposites. Samples with $C_{12}mim$ -MMT contents of 0.5, 1 and 2 wt% are designated as TM-CMMT0.5, TM-CMMT1 and TM-CMMT2, respectively.

Meanwhile, neat PMMA and a PMMA/AMMT nanocomposite with 2 wt% AMMT were also processed under the same conditions. After being dried at 60 °C under vacuum for 24 h, the neat PMMA and OM samples were injection-molded into specimens with dimensions of 60.0 × 12.8 × 1.8 mm for DMA using a Haake Instruments MicroInjector. The samples were also compression-molded into films of 300 μm thickness at 200 °C under vacuum, which were used for transmittance measurements. The molded samples were further dried at 60 °C under vacuum for 6 h to remove possible moisture.

Characterization

XRD measurements were conducted using an X-ray diffractometer (Rigaku D/MAX 2500) with Cu K α radiation (40 kV, 200 mA) between 2 and 20° (2θ) at a scanning rate of 3° min⁻¹. TEM images were acquired using a TEM instrument (JEOL 2200 FS) with an acceleration voltage of 200 kV. The samples for TEM analysis were prepared by microtoming 50–100 nm thick films from the nanocomposites with an ultramicrotome (Leica Ultracut R). The optical transmittance of the films was recorded using a UV-visible spectrophotometer (PERSEE TU-1901) in the wavelength range from 400 to 900 nm. Transmittance values of each film were collected on five points uniformly distributed on the sample, and then the mean value of transmittance was calculated. DMA measurements were performed using a TA DMA Q800 in dual cantilever mode at an oscillation frequency of 1.0 Hz. DMA data were recorded from room temperature to 160 °C at a heating rate of 3 °C min⁻¹. TGA was carried out with a PerkinElmer Pyris 1 from 50 to 800 °C at a heating rate of 10 °C min⁻¹ in a dry nitrogen environment. The compatibility of PMMA and $C_{12}mimPF_6$ was observed for samples freeze-fractured in liquid nitrogen and sputter-coated with gold using scanning electron microscopy (SEM, JEOL JSM-6700F).

RESULTS AND DISCUSSION

Microstructures of PMMA/MMT nanocomposites prepared by OM

In this study, the structure of nanocomposites and MMT at the nanometer scale was characterized using XRD patterns and TEM images, which can show directly the dispersion of MMT layers after intercalation of organic cations and polymer chains.

The XRD patterns of OM samples are shown in Fig. 1(a), and those of Na-MMT, $C_{12}mim$ -MMT and TM samples are shown in Fig. 1(b) for comparison. Both OM-MMT2-IL2.5 and OM-MMT1-IL2.5 exhibit a narrow diffraction peak at $2\theta = 2.8^\circ$, while Na-MMT shows a peak at $2\theta = 9.0^\circ$. The interlayer spacing of MMT has increased markedly from 0.98 nm in Na-MMT to 3.18 nm in OM samples, which is also larger than those of $C_{12}mim$ -MMT (1.73 nm) and TM samples (2.74 nm). Accordingly, as demonstrated in Figs 2(a) and (b), the platelets in both OM samples consist of multilayers and exhibit intercalated microstructure. During the melt blending, both $C_{12}mimPF_6$ molecules/ $C_{12}mim$ cations are suggested to diffuse into the galleries of Na-MMT. Consequently, the conversion of the hydrophilic surface of MMT layers to a hydrophobic surface and the subsequent intercalation of PMMA into the hydrophobic galleries take place in one pot to form orderly intercalated nanocomposites.

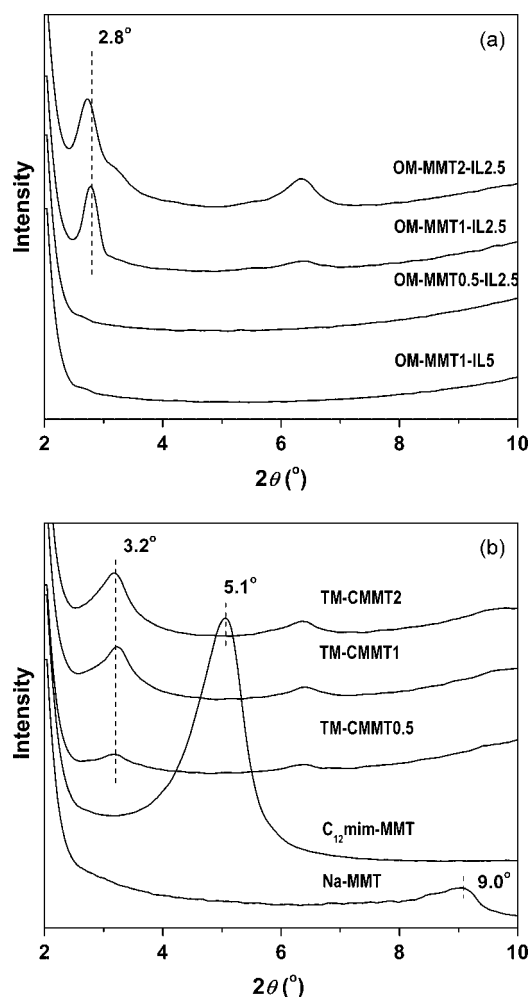


Figure 1. XRD patterns of (a) one-pot nanocomposites and (b) Na-MMT, C₁₂mim-MMT and two-step nanocomposites.

Moreover, the addition of C₁₂mimPF₆ in the preparation of OM-MMT2-IL2.5 and OM-MMT1-IL2.5 is in large excess over the amount needed to modify Na-MMT (more than three times the CEC of Na-MMT). The ionic nature of the ionic liquid may result in strong attractive interaction with MMT layers, and facilitate intercalation of C₁₂mimPF₆ molecules into the galleries of MMT. Some intercalated organic salts would take part in the ion-exchange reaction between Na⁺ and C₁₂mim cations, while others may be adsorbed by the MMT layer via electrostatic interaction.^{23,36,37} Therefore, the one-pot method proposed in this study is more effective than the standard two-step method to prepare nanocomposites from Na-MMT directly.

The marked expansion of Na-MMT galleries in OM nanocomposites is also ascribable to the high compatibility of C₁₂mimPF₆ with PMMA. Figure 3 shows SEM images of the PMMA/C₁₂mimPF₆ blends. It is seen clearly that the morphology of the fractured surface is very homogeneous, and no obvious dispersed phase is observed for the blend containing up to 10 wt% of ionic liquid. This result is well consistent with previous studies, where alkyimidazolium hexafluorophosphate ionic liquids were found to be excellent plasticizers for PMMA.^{34,35} Therefore, the intercalated C₁₂mimPF₆ facilitates the diffusion of PMMA chains into the galleries of MMT to expand their spacing with the assistance of strong shear and high temperature in the melt blending. Moreover, the

MMT layers decorated with C₁₂mimPF₆ *in situ* are more compatible with PMMA than C₁₂mim-MMT, resulting in the larger interlayer spacing for the MMT in OM nanocomposites than in the nanocomposites prepared by the standard two-step melt-blending method.

As for the OM-MMT0.5-IL2.5 sample, diffraction peaks disappear in the 2θ range between 2° and 10°, as shown in Fig. 1(a). By comparison, a small but obvious peak is observed for the TM-CMMT0.5 sample containing the same content of MMT (Fig. 1(b)). The absence of characteristic peaks of MMT in the XRD pattern indicates that MMT is nearly exfoliated and dispersed in the sample with interlayer spacing not less than 4.43 nm (according to 2θ = 2°). TEM images further validate the exfoliated structure of the MMT, as evident from Fig. 2(c). This is probably because of the large amount of excess C₁₂mimPF₆ (up to 16 times the CEC) in OM-MMT0.5-IL2.5. A PMMA/MMT nanocomposite, OM-MMT1-IL5, was also prepared using the one-pot method, which has the same ratio of C₁₂mimPF₆ to Na-MMT as OM-MMT0.5-IL2.5 but greater Na-MMT content of 1 wt%. The dispersion of MMT layers in OM-MMT1-IL5 is consistent with that in OM-MMT0.5-IL2.5, as validated by the XRD pattern (Fig. 1(a)) and TEM image (Fig. 2(d)). This indicates that the microstructure of the nanocomposites obtained is determined primarily by the amount of C₁₂mimPF₆. Large excess of C₁₂mimPF₆ extensively expands the MMT layer spacing, and facilitates the further diffusion of PMMA to separate the layers due to the high compatibility of C₁₂mimPF₆ with the polymer matrix.

In the one-pot method, the hydrophilic Na-MMT is decorated with alkyimidazolium-based ionic liquid *in situ* during melt blending. It is more efficient and feasible in comparison with the time-consuming standard two-step method for the preparation of polymer nanocomposites with a prior ion-exchange procedure.^{23,38} Furthermore, the obtained hydrophobic galleries of MMT favor the intercalation of polymer chains to further enlarge the interlayer spacing. Therefore, better intercalation and even exfoliation of MMT can be obtained in OM nanocomposites, as shown in Fig. 1(a).

Microstructures of PMMA/MMT nanocomposites prepared by TM

The PMMA nanocomposites prepared by TM, i.e. Na-MMT was modified using the standard ion-exchange technique before it was blended with PMMA, were characterized as a comparison.

As shown in Fig. 1(b), all TM nanocomposites display similar XRD patterns in the 2θ range 2–10°. The diffraction peak shifts from 2θ = 5.1° corresponding to 1.73 nm for C₁₂mim-MMT to 2θ = 3.2° corresponding to 2.74 nm after melt intercalation, indicating an enlarged interlayer spacing. The modification of Na-MMT renders the layer surface organophilic and improves the compatibility with polymer, which facilitates the further intercalation of polymer chains during melt blending. The diffusion of PMMA chains into C₁₂mim-MMT galleries results in the formation of intercalated PMMA nanocomposites.

Physical and mechanical properties of PMMA/MMT nanocomposites prepared by OM

The dispersion of high-aspect-ratio MMT platelets in PMMA matrix at the nanoscale, which is confirmed by XRD patterns, would result in dramatic enhancements in physical and mechanical properties of the OM nanocomposites compared to neat PMMA.

Optical properties

Figure 4 shows digital photos of various samples in front of the logo of the Institute of Chemistry, Chinese Academy of

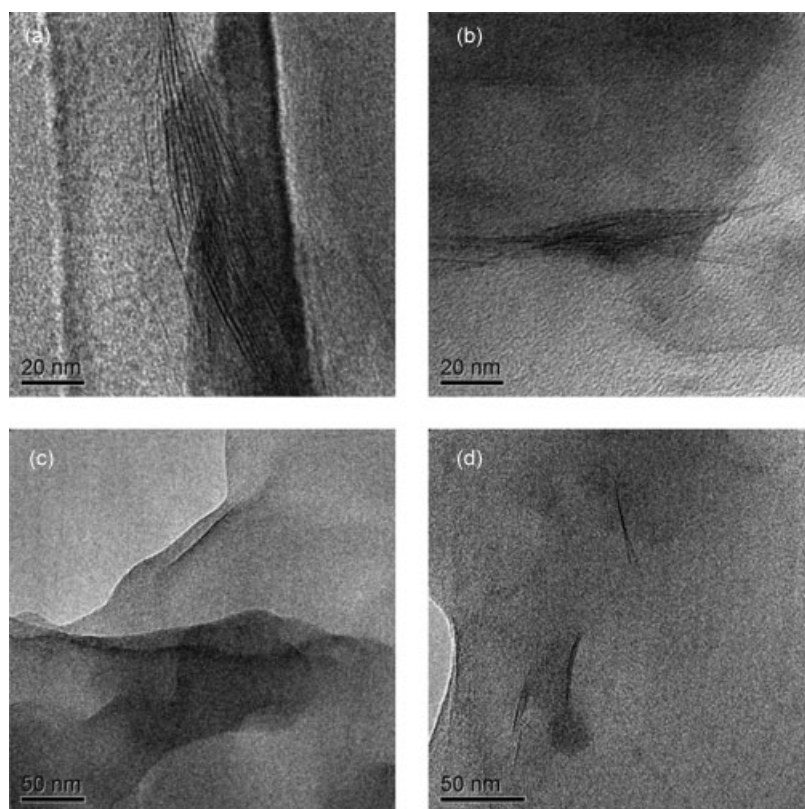


Figure 2. TEM images of (a) OM-MMT2-IL2.5, (b) OM-MMT1-IL2.5, (c) OM-MMT0.5-IL2.5 and (d) OM-MMT1-IL5.

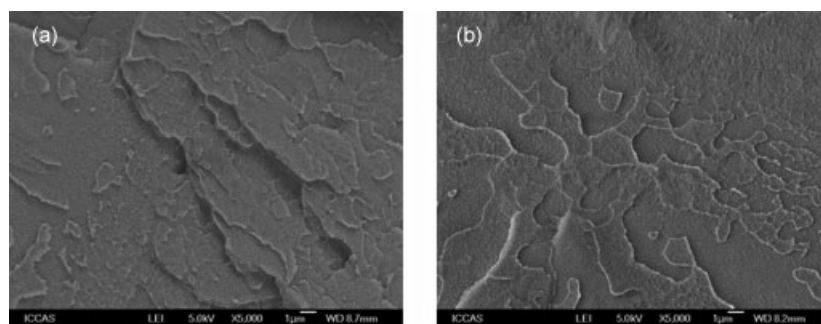


Figure 3. SEM micrographs of fractured surfaces of (a) PMMA/ C_{12} mimPF₆ (2.5 wt%) and (b) PMMA/ C_{12} mimPF₆ (10 wt%) samples.

Sciences. By visual inspection, the homogeneous OM samples have high optical transparency similar to neat PMMA, which is generally accepted as a transparent material. On the contrary, the PMMA/Na-MMT composite prepared by melt blending exhibits obvious aggregation of Na-MMT in the transparent polymer matrix. Therefore, the OM nanocomposites films were further characterized using UV-visible spectroscopy along with neat PMMA film as reference.

The transmittance values of neat PMMA and OM film samples at a wavelength of 800 nm were recorded and are given in Table 1. OM-IL2.5 film displays almost the same transmittance as the neat PMMA film, indicating the addition of C_{12} mimPF₆ does not decrease the optical transparency of PMMA matrix due to their good compatibility. With the addition of Na-MMT, the transmittance remains high for nanocomposite films up to 1 wt% of Na-MMT (OM-MMT0.5-IL2.5 and OM-MMT1-IL2.5). On increasing the Na-MMT content to 2 wt%, OM-MMT2-IL2.5 film still has a

relatively high transmittance of $85.6 \pm 0.6\%$. These results indicate the agglomeration only at the nanoscale formed from MMT layers and the good dispersion in the polymer matrix with the assistance of C_{12} mimPF₆. This further confirms the efficiency of the one-pot method for the preparation of polymer nanocomposites.

Dynamic mechanical properties

The thermomechanical properties of the OM samples were characterized using DMA with neat PMMA as comparison. The storage modulus (G') as a function of temperature and T_g were obtained during the characterization.

G' of the samples is plotted for the temperature range from 30 to 165 °C in Fig. 5. G' is related to the ability of a material to store mechanical energy during deformation. At temperatures below about 100 °C, all the samples have high modulus, which is observed to decrease slowly with increasing temperature. Above 110 °C, G' decreases steeply with an increase of temperature,



Figure 4. Digital photos of (a) neat PMMA, (b) OM-IL2.5, (c) OM-MMT1-IL2.5 and (d) OM-MMT2-IL2.5 samples in front of ICCAS logo.

	Neat PMMA	OM-IL2.5	OM-MMT0.5-IL2.5	OM-MMT1-IL2.5	OM-MMT2-IL2.5
Transmittance (%) ^a	89.7 ± 0.9 ^b	89.1 ± 0.5 ^b	90.0 ± 0.3 ^b	89.8 ± 0.5 ^b	85.6 ± 0.6 ^b
T_g (°C)	122.4	117.7	118.1	120.5	122.7
T_d (°C)	341.2	346.3	346.7	348.1	349.1

^a Transmittance at 800 nm obtained from UV-visible spectra.
^b $X \pm Y$: X indicates the mean of the transmittance values of five sample points, while Y is the variance.

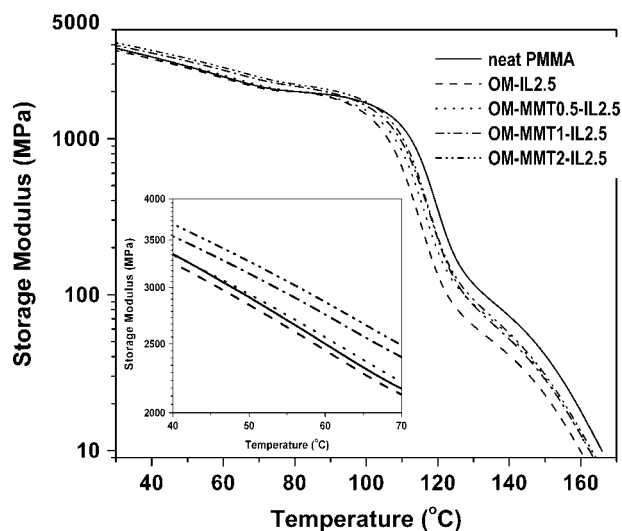


Figure 5. Storage modulus versus temperature for neat PMMA and one-pot samples.

indicating the samples lose their stiffness quickly due to the glassy to rubbery state transition. OM-IL2.5 exhibits a smaller G' relative to neat PMMA in the whole temperature range studied because of the plasticization effect of $C_{12}mimPF_6$, which is consistent with previous studies. In contrast, G' increases with further addition of Na-MMT up to 2 wt%, resulting from the high stiffness of the inorganic filler. For example, the storage modulus of OM samples at 60 °C increases from 2.45 GPa for OM-IL2.5, to 2.55 GPa for OM-MMT0.5-IL2.5, 2.75 GPa for OM-MMT1-IL2.5 and 2.86 GPa for OM-MMT2-IL2.5. In the low-temperature region, the loading of 0.5 wt% MMT nearly offsets the loss of storage modulus by 2.5 wt% of $C_{12}mimPF_6$, and OM-MMT1-IL2.5 exhibits higher G' than neat PMMA. However, in the high-temperatures region, G' of all OM nanocomposites is smaller than that of neat PMMA. This is probably attributable to the quickly decreasing modulus of polymer matrix in the presence of excess $C_{12}mimPF_6$, which would be in the liquid state at these temperatures.

Table 1 shows T_g obtained from the peak temperature of loss angle tangent ($\tan \delta$) for neat PMMA and OM samples. It is observed that the $\tan \delta$ peak shifts to lower temperatures with addition of $C_{12}mimPF_6$, and then to higher temperatures with increasing loading of Na-MMT, compared to neat PMMA. When the Na-MMT content is 2 wt%, T_g of OM-MMT2-IL2.5 is equal to that of neat PMMA. The excess $C_{12}mimPF_6$ is responsible for the decrease of T_g for the OM samples. Therefore, these results are consistent with those for G' , indicating that the well-dispersed MMT layers and excess compatible $C_{12}mimPF_6$ have opposite effects on the mobility of polymer chains. Moreover, these effects also similarly influence the mechanical properties, e.g. tensile strength and impact strength, of these nanocomposites (data not shown here).

Thermal stability

In this study, an alkylimidazolium-based ionic liquid was used as the organic modifier of Na-MMT mainly due to the better thermal stability of imidazolium cations than alkylammonium ones. In order to study the interaction between $C_{12}mim$ cations and MMT layers, TGA analysis was applied. Figure 6 shows the TGA and derivative thermogravimetry (DTG) curves of $C_{12}mim$ -MMT along with pristine Na-MMT and two ionic liquids in nitrogen atmosphere. The mass loss of Na-MMT occurs from 500 to 750 °C and has a maximum rate at about 681 °C, which is due to the dehydroxylation of the aluminosilicate lattice. However, $C_{12}mim$ -MMT exhibits two discrete decomposition events between 250 and 500 °C, indicating the degradation of organic components, while the organic modifier $C_{12}mimBr$ used for preparing $C_{12}mim$ -MMT displays single-step decomposition between 200 and 350 °C with the DTG peak at about 299 °C (Fig. 6(b)). Consequently, both decomposition events for $C_{12}mim$ -MMT have higher temperatures related to the maximum rate of mass loss than that of $C_{12}mimBr$. These results indicate that the presence of MMT layers with nanosized spacing influences the degradation process, products and kinetics of organic component therein. These two events might be assigned to two molecular environments of $C_{12}mimBr/C_{12}mim$ cations in MMT layers. The mass loss at 371 °C can be attributed to the $C_{12}mimBr$ molecules physically adsorbed onto the surface of MMT layers, while that

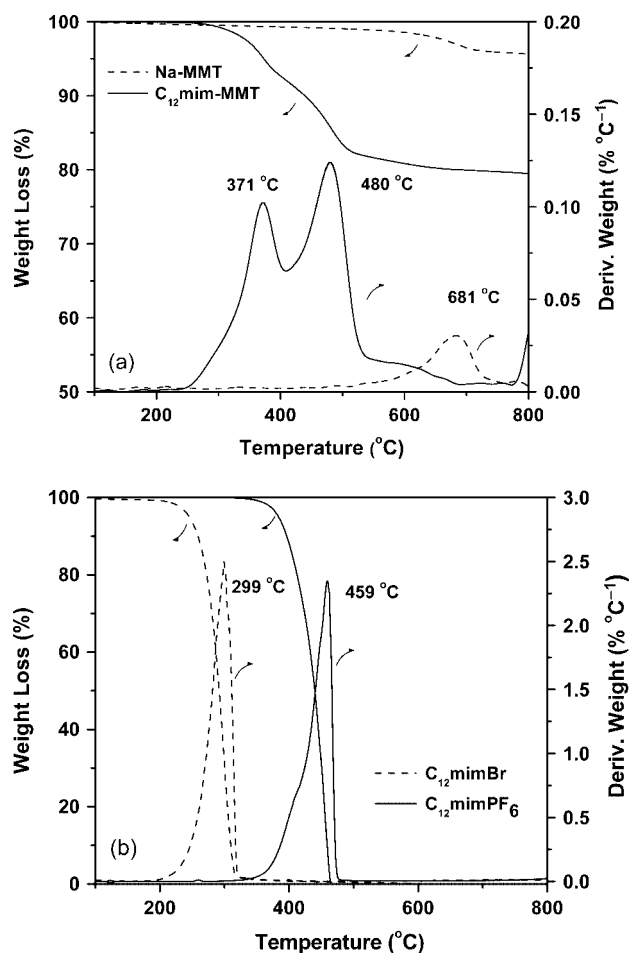


Figure 6. TGA and DTG curves of (a) Na-MMT and C_{12} mim-MMT, and (b) C_{12} mimBr and C_{12} mimPF₆.

at 480 °C to C_{12} mim cations tethered to the surface via cation-exchange reaction. The latter has stronger interaction with MMT layers than the former, resulting in higher thermal stability.

The OM samples together with neat PMMA were also characterized using TGA. The thermal decomposition temperature (T_d) at 5% weight loss was used to represent the thermal stability of the samples. T_d values for various samples are given in Table 1. T_d increases from 341 °C for neat PMMA to 346 °C for OM-IL2.5, most probably due to the high thermal stability of C_{12} mimPF₆. As shown in Fig. 6(b), T_d of C_{12} mimPF₆ is 384 °C. Moreover, the presence of Na-MMT further shifts T_d to higher temperatures, i.e. to 347–349 °C for OM nanocomposites. Therefore, both C_{12} mimPF₆ and MMT improve the thermal stability of the nanocomposites. By comparison, PMMA/AMMT exhibits T_d of 333 °C, which is 8 °C lower than that of neat PMMA and 16 °C lower than that of OM-MMT2-IL2.5. This confirms that the low decomposition temperature of the alkylammonium cations decreases the thermal stability of the PMMA/alkylammonium-treated MMT sample. Therefore, alkylimidazolium-based ionic liquids have an advantage for the preparation of thermally stable polymer/MMT nanocomposites.

CONCLUSIONS

A new one-pot method was proposed in this study to prepare transparent PMMA/MMT nanocomposites. Using this method, the

hydrophilic Na-MMT layers were decorated with hydrophobic C_{12} mimPF₆ ionic liquid *in situ* during 10 min melt blending with PMMA, where the intercalation of polymer chains took place subsequently. Accordingly, the method has the distinct advantage of greater efficiency than the time-consuming standard ion-exchange procedure for Na-MMT modification. As a potential additive for polymer materials, excess C_{12} mimPF₆ remained in the nanocomposites, further leading to larger interlayer spacing, as revealed by XRD analysis. Moreover, the presence of well-dispersed MMT layers and compatible C_{12} mimPF₆ in PMMA endows the obtained PMMA/MMT nanocomposites with high optical transparency and thermal stability. The bulk stiffness and chain mobility of the nanocomposites are determined by the combination of the plasticization effect from C_{12} mimPF₆ and the reinforcement effect from MMT layers at the nanoscale.

ACKNOWLEDGEMENT

This work was supported by the National Natural Science Foundation of China, grant no. 50873113.

REFERENCES

- 1 Ray SS and Okamoto M, *Prog Polym Sci* **28**:1539–1641 (2003).
- 2 Kojima Y, Usuki A, Kawasumi M, Okada A, Fukushima Y, Kurauchi T, et al, *J Mater Res* **8**:1185–1189 (1993).
- 3 Gilman JW, *Appl Clay Sci* **15**:31–49 (1999).
- 4 Gilman JW, Jackson CL, Morgan AB and Harris R, *Chem Mater* **12**:1866–1873 (2000).
- 5 Messersmith PB and Giannelis EP, *J Polym Sci A: Polym Chem* **33**:1047–1057 (1995).
- 6 Tong X, Zhao HC, Tang T, Feng ZL and Huang BT, *J Polym Sci A: Polym Chem* **40**:1706–1711 (2002).
- 7 Ray S, Galgali G, Lele A and Sivaram S, *J Polym Sci A: Polym Chem* **43**:304–318 (2005).
- 8 Wang Z and Pinnavaia TJ, *Chem Mater* **10**:1820–1826 (1998).
- 9 Ke YC, Long CF and Qi ZN, *J Appl Polym Sci* **71**:1139–1146 (1999).
- 10 Okamoto M, Morita S, Taguchi H, Kim YH, Kotaka T and Tateyama H, *Polymer* **41**:3887–3890 (2000).
- 11 Zheng X and Wong SC, *Compos Sci Technol* **63**:225–235 (2003).
- 12 Hsueh HB and Chen CY, *Polymer* **44**:1151–1161 (2003).
- 13 Chang JH, An YU, Cho D and Giannelis EP, *Polymer* **44**:3715–3720 (2003).
- 14 Magaraphan R, Lilayuthalert W, Sirivat A and Schwank JW, *Compos Sci Technol* **61**:1253–1264 (2001).
- 15 Tseng CR, Wu JY, Lee HY and Chang FC, *Polymer* **42**:10063–10070 (2001).
- 16 Vaia RA, Vasudevan S, Krawiec W, Scanlon LG and Giannelis EP, *Adv Mater* **7**:154–156 (1995).
- 17 Cho JW and Paul DR, *Polymer* **42**:1083–1094 (2001).
- 18 Vaia RA, Ishii H and Giannelis EP, *Chem Mater* **5**:1694–1696 (1993).
- 19 Liu LM, Qi ZN and Zhu XG, *J Appl Polym Sci* **71**:1133–1138 (1999).
- 20 Manias E, Touny A, Wu L, Strawhecker K, Lu B and Chung TC, *Chem Mater* **13**:3516–3523 (2001).
- 21 Drummy LF, Koerner H, Farmer K, Tan A, Farmer BL and Vaia RA, *J Phys Chem B* **109**:17868–17878 (2005).
- 22 Madaleno L, Thomsen JS and Pinto JC, *Compos Sci Technol* **70**:804–814 (2010).
- 23 Xi YF, Frost RL, He HP, Klopogge T and Bostrom T, *Langmuir* **2**:8675–8680 (2005).
- 24 Nah C, Han SH, Lee JH, Lee MH and Chung KH, *Polym Int* **53**:891–897 (2004).
- 25 Ngo HL, LeCompte K, Hargens L and McEwen AB, *Thermochim Acta* **357–358**:97–102 (2000).
- 26 Awad WH, Gilman JW, Nyden M, Harris RH, Sutto TE, Callahan J, et al, *Thermochim Acta* **409**:3–11 (2004).
- 27 Wang ZM, Chung TC, Gilman JW and Manias E, *J Polym Sci B: Polym Phys* **41**:3173–3187 (2003).
- 28 Gilman JW, Awad WH, Davis RD, Shields J, Harris RH, Davis C, et al, *Chem Mater* **14**:3776–3785 (2002).

- 29 Kim NH, Malhotra SV and Xanthos M, *Microporous Mesoporous Mater* **96**:29–35 (2006).
- 30 Langat J, Bellayer S, Hudrlik P, Hudrlik A, Maupin PH, Gilman JW, et al, *Polymer* **47**:6698–6709 (2006).
- 31 Livi S, Rumeau JD, Pham TN and Gérard JF, *J Colloid Interface Sci* **349**:424–433 (2010).
- 32 Ding YS, Zhang XM, Xiong RY, Wu SY, Zha M and Tang HO, *Eur Polym J* **44**:24–31 (2008).
- 33 Byrne C and McNally T, *Macromol Rapid Commun* **28**:780–784 (2007).
- 34 Scott MP, Brazel CS, Benton MG, Mays JW, Holbrey JD and Rogers RD, *Chem Commun* **13**:1370–1371 (2002).
- 35 Scott MP, Rahman M and Brazel CS, *Eur Polym J* **39**:1947–1953 (2003).
- 36 Xi YF, Ding Z, He HP and Frost RL, *J Colloid Interface Sci* **277**:116–120 (2004).
- 37 Klapysa Z, Fujita T and Iyi N, *Appl Clay Sci* **19**:5–10 (2001).
- 38 Vazquez A, López M, Kortaberria G, Martín L and Mondragon I, *Appl Clay Sci* **41**:24–36 (2008).